

Modeling of plasma dynamics in the inner geospace during enhanced magnetospheric activity



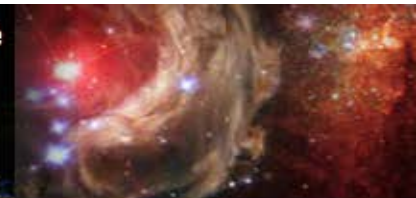
<http://proteus.space.noa.gr/~hnswrn>



C. Tsironis¹, A. Anastasiadis¹, C. Katsavrias^{2,1}, I. A. Daglis²

¹*National Observatory of Athens, Greece*

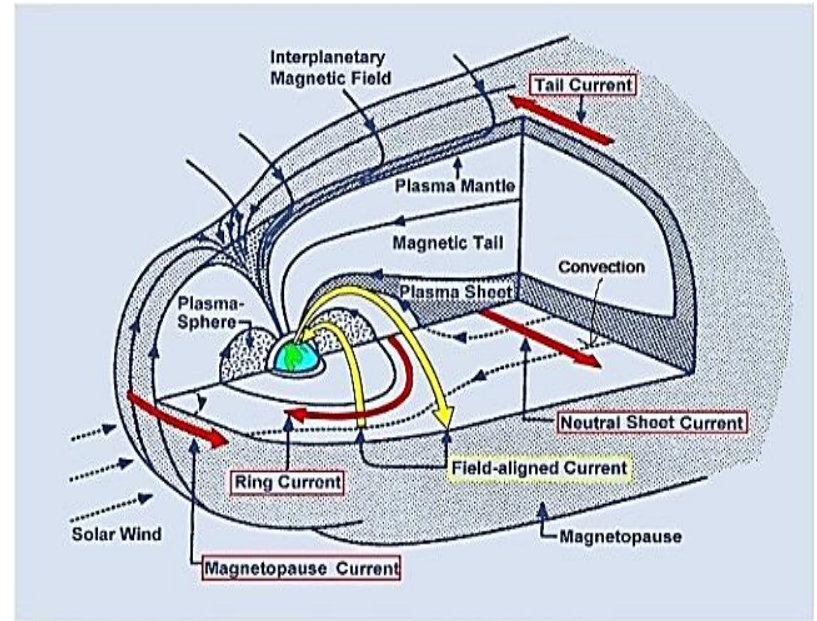
²*National and Kapodestrian University of Athens, Greece*



Objectives of our research

■ Motivation and milestones

- *Model for the near-Earth plasma response to geoeffective events*
 - Goal: Space weather prediction
 - Final link in the Sun-to-Earth analysis of solar eruptions (Patsourakos et al 2015)
- *Focus on ring current dynamics*
 - Origin and transport of RC ions during storms and substorms
 - Interaction with other sources
 - Correlation with event's phases



■ Requirements for building a physics-based model

- *Description of the electric and the magnetic field in geospace*
- *Computation of the plasma dynamics in the inner magnetosphere*
- *Utilization of the data from the numerical computations*
 - Estimation of the associated geomagnetic indices (K_p , $Dst/Sym-H...$)
 - Comparison with ground-based and satellite/spacecraft measurements



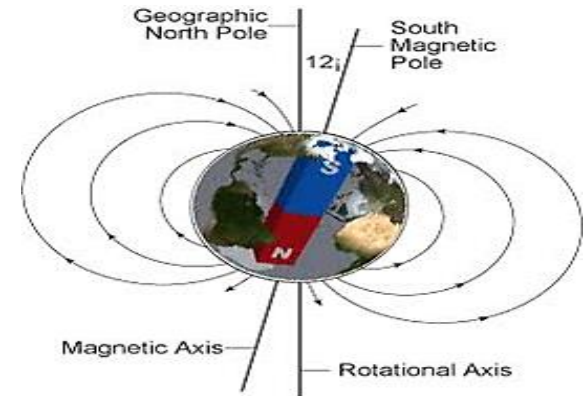
Model for the geomagnetic field

■ B-field in the inner magnetosphere:

- *Tilted dipole* (Earth's physical magnet)

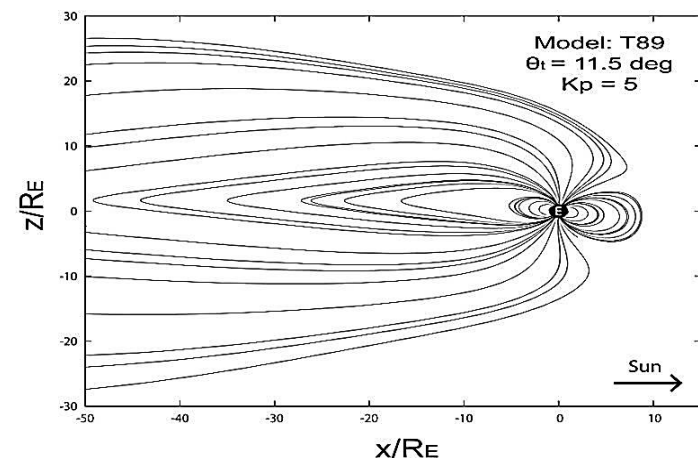
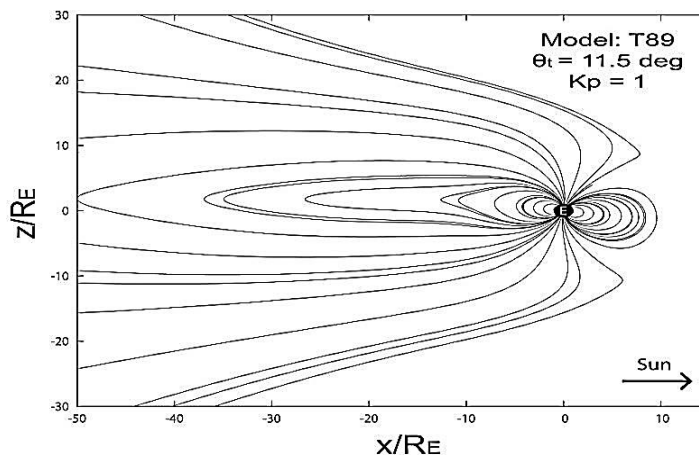
$$\mathbf{B}_{\text{dip}} = \frac{\mu_0 M_{\text{dip}}}{4\pi r^3} [3(\hat{\mathbf{m}}_{\text{dip}} \cdot \hat{\mathbf{r}})\hat{\mathbf{r}} - \hat{\mathbf{m}}_{\text{dip}}]$$

- *External field* (RC, magnetopause & tail)
 - *Tsyganenko model of 1989 (T89)*
 - Input: Tilt angle, *Kp* index



■ Visualization of B → Field-line tracing

- Benchmark with T96-TS05: Minor deviations in the simulated region



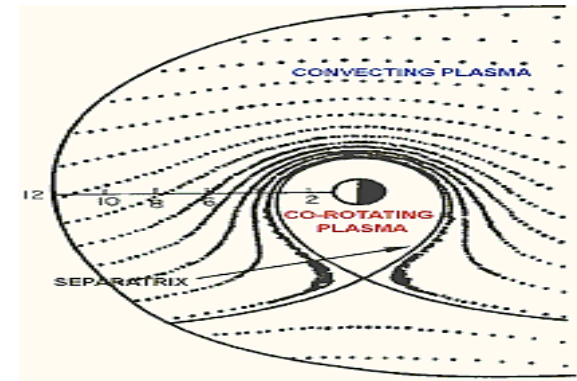
Model for the electric field

■ E-field in the inner magnetosphere:

- Plasma convection and corotation
 - Volland-Stern-Maynard-Chen model (VSMC)

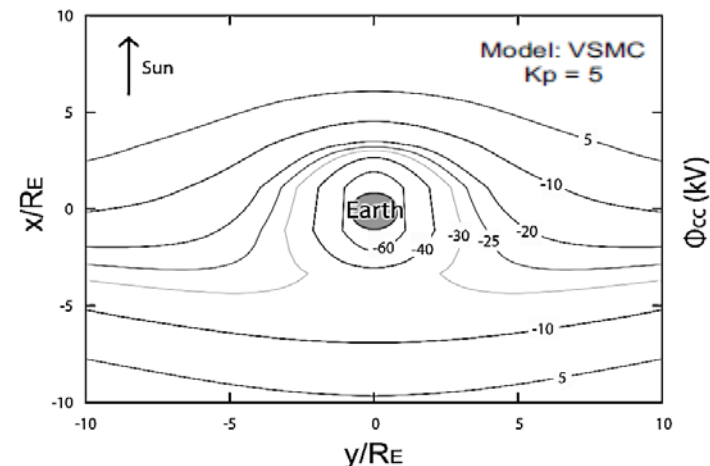
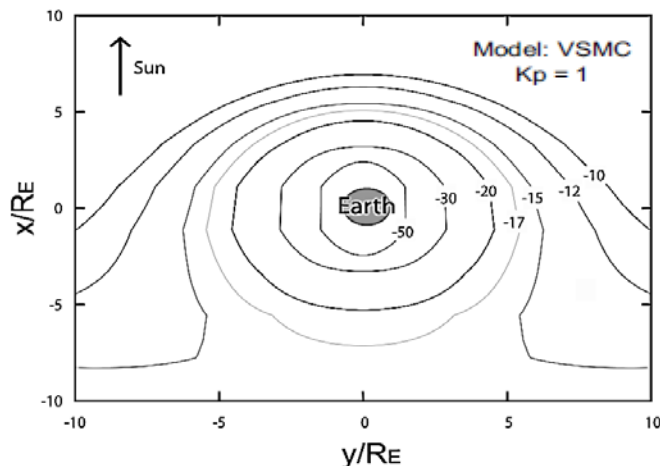
$$\Phi_{cc} = \frac{v_1}{(v_2 Kp^2 + v_3 Kp + 1)^3} \cdot \frac{y r^{\gamma-1}}{R_E^\gamma} - \frac{\omega_E B_E R_E^3}{r}$$

- Magnetic induction (Faraday's law)
 - Generated by the Sun-driven variation of **B**



■ Visualization of E_{cc} → Equipotential contours

- Benchmark with BRH97/WM05: Deviation only in the pause and far tail



Dynamic variation of the fields

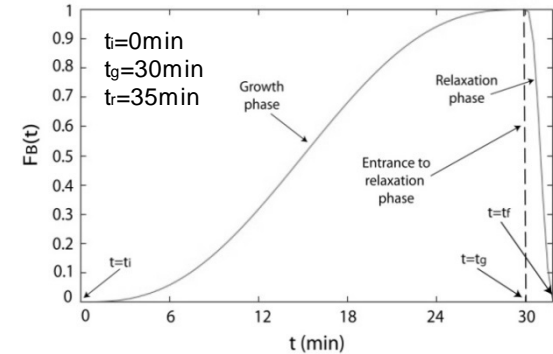
■ Event-based description of $B(t)$, $E(t)$

□ Disturbances in the ion motion time-scale

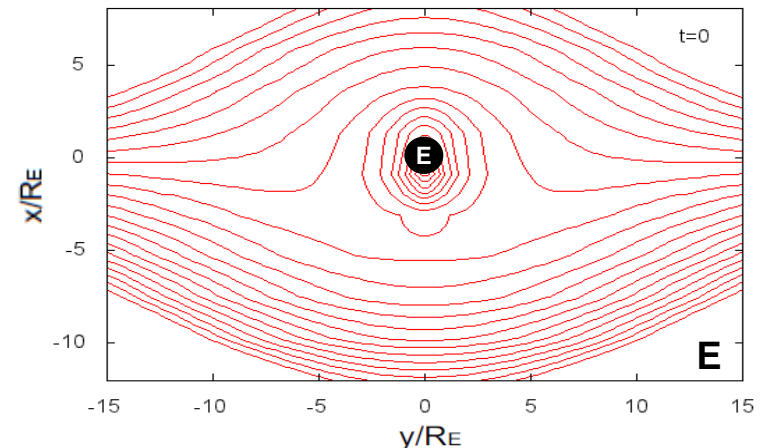
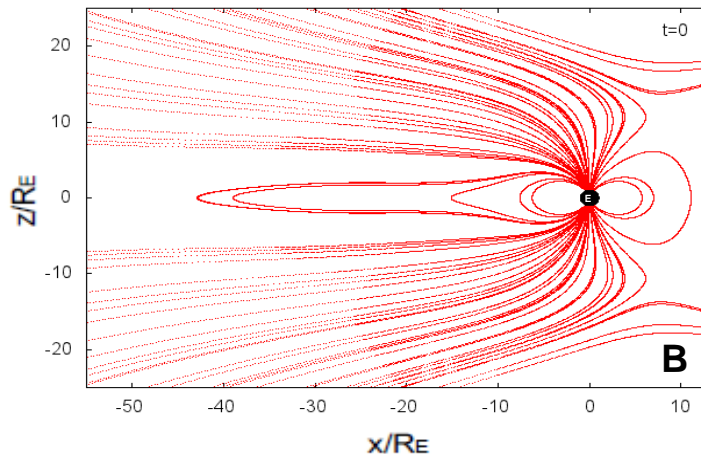
$$\frac{\partial B_{\text{ext}}}{\partial t} = \sum_j \left(\frac{\partial B_{\text{ext}}}{\partial G_j} \cdot \frac{dG_j}{dt} \right) \longrightarrow B(\mathbf{r}, t) = B_{\text{dip}}(\mathbf{r}) + B_{\text{ext}}[\mathbf{r}, G_j(t_i)] + F_B(t) \cdot \{B_{\text{ext}}[\mathbf{r}, G_j(t_f)] - B_{\text{ext}}[\mathbf{r}, G_j(t_i)]\}$$

- F_B defined according to observed event scales:
Set-off at $t=t_i$, peak at $t=t_g$ and restoration at $t=t_r$
- G depends on the B -field model ($[\theta_t, K_p]$ for T89)

□ The electric field is defined accordingly $\rightarrow E(\mathbf{r}, t) = -\nabla\Phi_{cc}(\mathbf{r}, t) - \frac{\partial A_{\text{ext}}(\mathbf{r}, t)}{\partial t}$



■ A substorm's tale: $t_i=0$, $t_g=35m$, $t_r=40m$ - $\theta_t=0$, $K_p=1 \leftrightarrow 5$



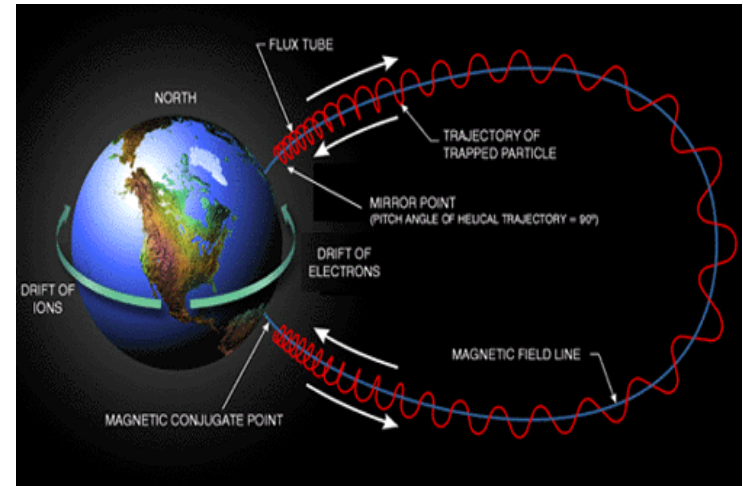
Model for the ion trajectories

■ Overview of test-particle code

- Geomagnetic field: T89 model
- C&C electric field: VSMC model
 - + Induced field = Total electric field
- Motion equations: Lorentz forcing

$$m \frac{d^2 \mathbf{r}}{dt^2} = q \left(\mathbf{E} + \frac{d\mathbf{r}}{dt} \times \mathbf{B} \right) + m\mathbf{g}$$

- GC approximation (cutoff criterion):
Deviations when AIs are broken

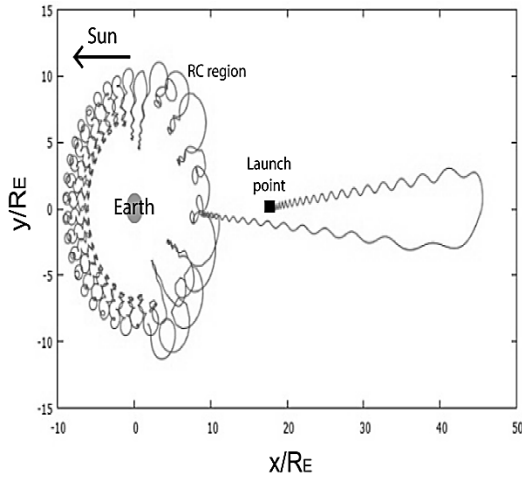


■ Setup of the test-particle computations

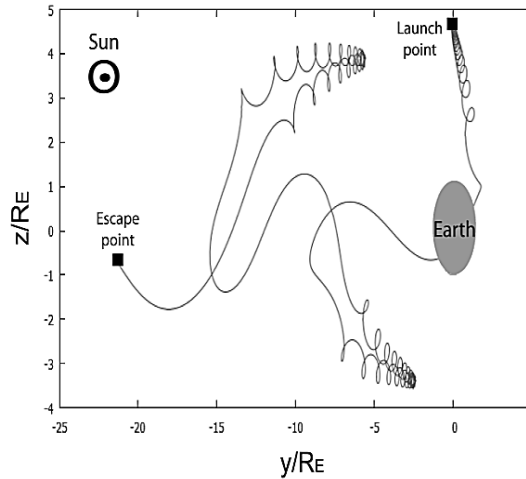
- Initial conditions: Ions launched at $t_0 = -8\text{min}$ and move until $t_f - t_i \approx 3\text{h}$
 - Ion species: (I)+(II) O^+ (amu=16), H^+ (amu=1)
 - Kinetic energy $E_k(t_0)$: (I) 4KeV, 7KeV, 0.5KeV, (II) [0.5-20] KeV
 - Coordinates $r(t_0), \varphi(t_0), \theta(t_0)$: (I) 20 R_E , (II) [2,30] R_E , (I)+(II) 24h, 25°
 - Velocity pitch angle $\alpha(t_0)$: (I)+(II) 90°
- Numerical computations are performed for two purposes
 - [Part I] Exploration of different orbit types (trapped, escape, precipitating)
 - [Part II] Dependence of the ion dynamics on the initial conditions



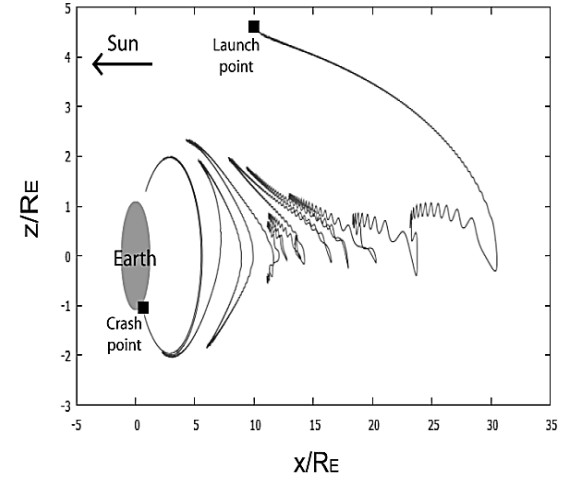
Results from Part I (all species)



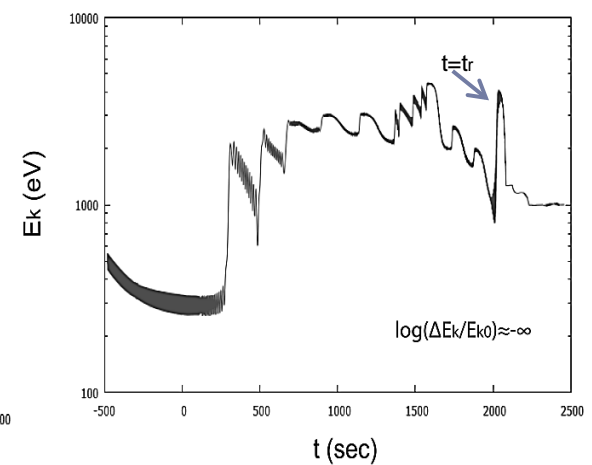
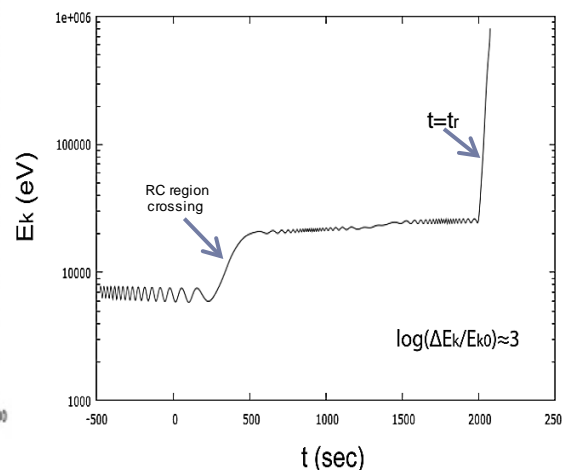
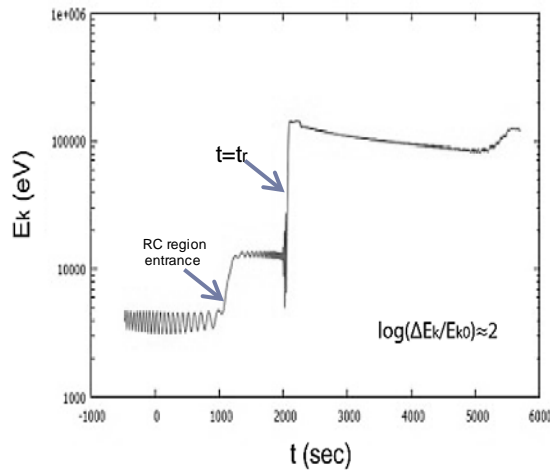
Trapped orbit (O^+)



Escape orbit (H^+)

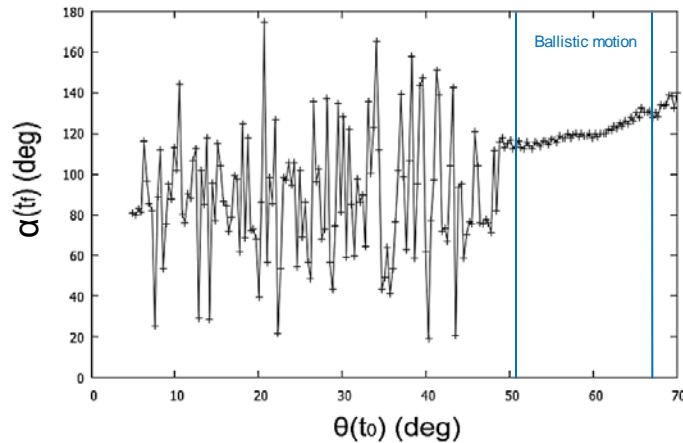


Precipitating orbit (H^+)

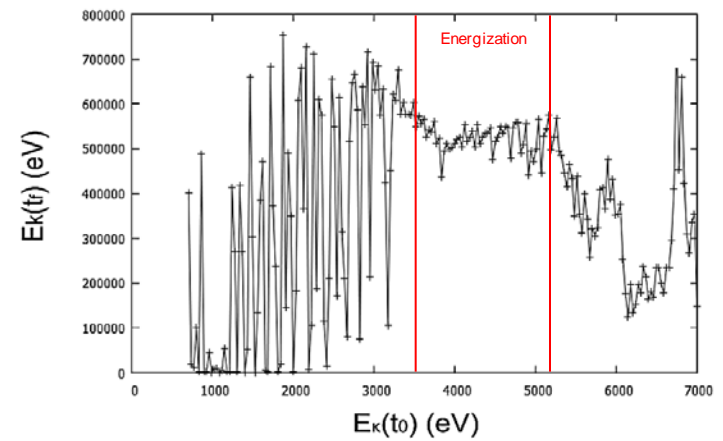


Results from Part II (only O⁺)

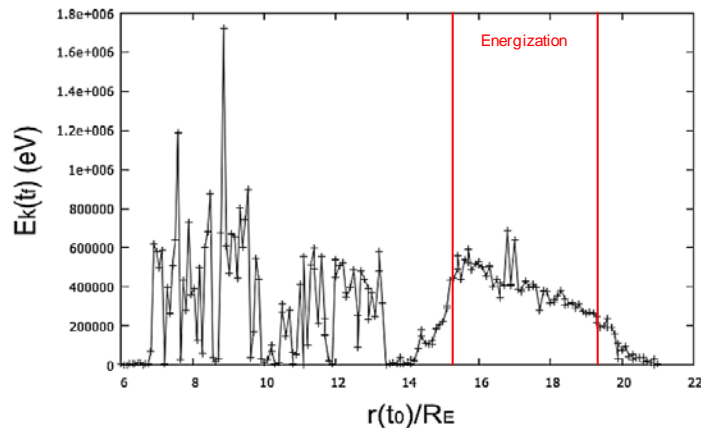
Pitch angle dependence on latitude



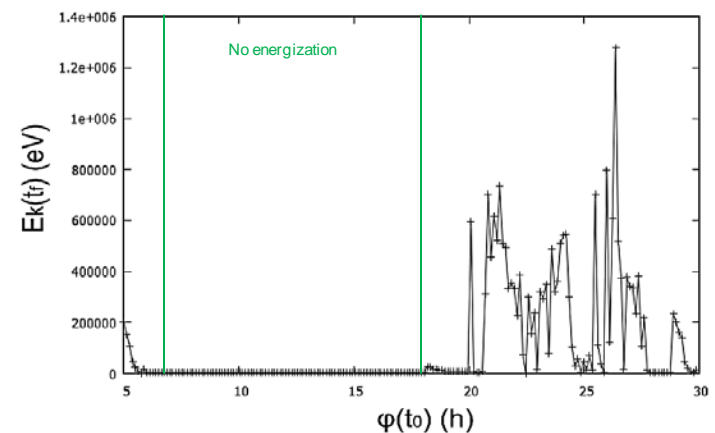
Acceleration dependence on energy



Acceleration dependence on location



Acceleration dependence on MLT



Overview of results on dynamics

■ Test-particle orbits reveal fragments of the RC dynamics

- *O⁺ ions launched from the plasma sheet are driven towards Earth during the disturbance and get trapped in the ring current*
 - Acceleration is stronger during the substorm relaxation phase ($t_g < t < t_r$)
 - Similar behavior in latitudes from $\pm 5^\circ$ to $\pm 25^\circ$ → See poster [S1.24](#)
- *High latitude H⁺ ions launched from the PS are not trapped in the RC*
 - Different picture for low latitude particles → See poster [S1.24](#)

■ Analysis using ensembles of test particles

- *Sensitive dependence of ion dynamics on the initial conditions*
 - Counteract: IC regions exhibiting specific trend(s) in phase-space kinetics
- *PS = Reservoir of O⁺ which enhance the RC energy in storm-time*
 - In quiet-time, H⁺ is the majority ion species in the ring current

■ Validation of the above results

- *Estimate the statistical weight of each ion population (RC, near-Earth tail, precipitating and escape) per species*
 - 10⁴ high-latitude ions launched from PS

Ion type	N_{ens}	N_{rc}	N_{ntl}	N_{ter}	N_{esc}
O ⁺	10000	4596	2271	673	2460
H ⁺	10000	378	2414	3365	3843

10⁴ test ions, injected from the high-latitude PS, distributed to ring current (N_{rc}), near-Earth tail (N_{ntl}), precipitating (N_{ter}) and escaping (N_{esc})



Estimation of geomagnetic indices

■ Computation of the Dst index from ion kinematic data

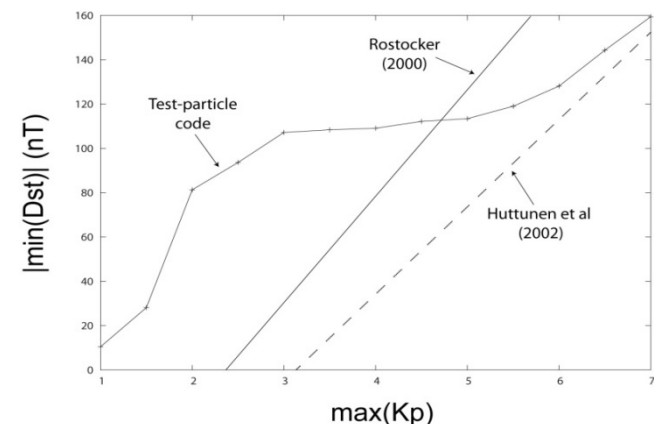
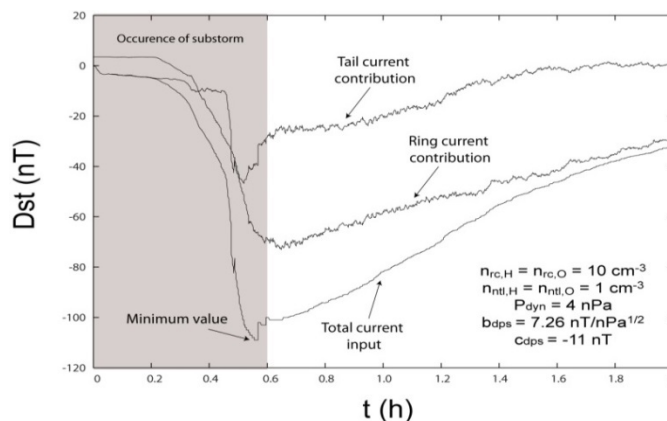
- Dessler-Parker-Sckopke (DPS) relation in test-particle simulations

$$Dst = -\frac{\mu_0}{2\pi B_E R_E^3} \sum_{pp} E_{pp} + b_{dps} \sqrt{P_{dyn}} + c_{dps} \quad E_{pp} = V_{pp} \sum_i n_{pp,i} \langle E_k \rangle_{pp,i} \quad V_{rc} = 2\pi^2 R_{rc} r_{rc}^2 \quad \text{and} \quad V_{ntl} = R_{ntl}^3 - V_{rc}$$

- RC region: Torus (R_{rc}, r_{rc}) containing equal portions (densities) of H^+ & O^+
- E_{pp} computed for ions travelling from the PS to the RC & near-Earth tail

■ Numerical results for Dst (+ comparisons)

- Contribution of tail current to Dst: ~30% (25% reported in literature)
- Benchmark with observations (Rostocker 2000; Huttunen et al. 2004)
 - Max(Kp) is modified from 1 to 7 → Minimum value of Dst is recorded



Concluding remarks

- **Analysis of substorm events using test particles**
 - *“Open-loop” study of ring & near-Earth tail current dynamics*
 - Model for the Sun-driven electric & magnetic field in the inner geospace
 - Computation of the ion motions in the disturbed magnetosphere
 - *Estimation of associated geomagnetic indices and their interrelations*
- **Workaround of approximations in our model**
 - *Kp-based description of the geomagnetic field during substorms may be partially in contrast to its global and averaged character*
 - Computed correlation of Kp & Dst connects to previous studies
 - *Use of the (older) T89 model for the disturbed magnetic field*
 - Benchmarks have shown only few differences in the region of interest
 - Use later Tij models → Numerical computation of **A** from **B** is required
- **Work currently under development**
 - *Benchmarking and verification against RBSP data (→ poster S1.24)*
 - Study injections during substorms with reverse-time test-particle simulations
 - *Inclusion of other “drivers” (forces) for the test particle dynamics*
 - Various types of electromagnetic waves (ULF, whistler, chorus, ...)